

Effect of Hydrogen on Corrosion Behavior of S32750 Super Duplex Stainless Steel

Yier Guo, Ping Liang*, Yanhua Shi, Yan Zhao, Fei Li, Lan Jin

School of Mechanical Engineering, Liaoning Shihua University, Fushun 113001, China

*E-mail: liangping770101@163.com

Received: 13 July 2018/ *Accepted:* 1 September 2018 / *Published:* 1 October 2018

Electrochemical behaviors and critical pitting temperature (CPT) of S32750 super duplex stainless steel (SDSS) in 3.5% NaCl solution with various hydrogen charging current densities (HCCD) were investigated by using open-circuit potential (OCP) curves, potentiodynamic polarization curves, electrochemical impedance spectroscopy (EIS), Mott-Schottky curves, and the potentiostatic polarization curves electrochemical measurements methods. Results showed that the open-circuit potential and self-corrosion potential gradually shift negatively, the passivity current density increases, pitting corrosion potential and self-corrosion potential decreases with the increase of the hydrogen charging current density from $10 \text{ mA}\cdot\text{cm}^{-2}$ to $100 \text{ mA}\cdot\text{cm}^{-2}$. Slope of the Mott-Schottky curves and the CPT gradually decreases as HCCD increased. As compared with the blank specimen, it is indicated that hydrogen leads to the delay of the passivation film formation and the reduction of the stability and integrity of the passivation film. The passivation film is more prone to cracking and dissolution, therefore, the corrosion of S32750 SDSS is more likely to occur after the hydrogen is charged.

Keywords: Hydrogen Charge Current Density, S32750 Super Duplex Stainless Steel, Critical Pitting Temperature

1. INTRODUCTION

The third-generation super duplex stainless steel (SDSS) S32750, which is low in C and high in N, Cr and other elements, displays excellent mechanical properties, welding properties and corrosion resistance, therefore, it is applied widely in marine equipment, seawater desalination and other aspects [1-3]. The presence of a large amount of Cl^- in the marine environment causes severe corrosion of marine equipment [4]. At present, the cathodic protection technology is employed for corrosion protection of marine steel structures and submarine pipelines worldwide, but when the potential of cathodic protection is overnegative, the precipitation of hydrogen may give rise to corrosion of

pipelines and other equipment, and sometimes leads to catastrophic results [5]. Recently, the concern has been put on the effect of hydrogen on the performance of duplex stainless steels. For example, Guo researched the effect of hydrogen on pitting susceptibility of 2507 duplex stainless steel [6], and it was found that hydrogen promoted the occurrence and growth of pitting corrosion, and pitting sensitivity increases with increasing hydrogen charging current density (HCCD). Zhao showed the effect of hydrogen on the stress corrosion cracking behavior of 2205 duplex stainless steel in a thin film of 3.5%NaCl solution [7], and the results reveal that although the electrochemical charge of hydrogen reduces the thickness of passive film, it does not affect the pitting behavior of 2205 duplex stainless steel. Therefore, it is indicated that the reason why hydrogen increases the stress corrosion sensitivity of 2205 duplex stainless steel is mainly the hydrogen embrittlement mechanism rather than the local anodic dissolution mechanism. Li investigated the effect of hydrogen filling on the pitting of duplex stainless steel by the scanning Kelvin probe force microscopy [8], and found that some low-potential regions appearing in the ferrite, austenite boundary, or ferrite phase of duplex stainless steel, may be the pitting preferential nucleation sites caused by hydrogen. So far, the study of S32750 SDSS has focused on the mechanical behavior, fatigue and welding performance [9-11]. However, there are relatively few studies on the effect of hydrogen on the corrosion behavior of S32750 SDSS.

The lowest temperature at which pitting corrosion occurs in this particular environment was called CPT. CPT can accurately reflect the sensitivity of materials to temperature. It is an important parameter to evaluate the pitting corrosion resistance of stainless steel and an important reference standard for select materials for corrosion resistance. However, so far, the effect of hydrogen on the CPT of S32750 SDSS almost has not been studied yet. Therefore, the influence of hydrogen on the corrosion behavior and CPT of S32750 SDSS in 3.5% NaCl solution is investigated by electrochemical impedance, potentiodynamic polarization, Mott-Schottky curves, and potentiostatic polarization methods.

2. EXPERIMENTAL

2.1 Material and test preparation

S32750 SDSS were used as the experimental material in this study, and whose chemical composition is presented in Table 1.

The microstructure was performed by a Leica QM500 optical microscope, as shown in Figure 1. It can be seen that the S32750 SDSS specimen is mainly composed of ferrite and austenite phase with an approximate volume ratio of 1:1 with the two phases uniformly distributed at regular intervals.

Table 1. Chemical composition of S32750 SDSS in this study (mass%)

Steel	C	Cr	Ni	Mo	N	Si	Mn	P	S	Fe
S32750 SDSS	0.021	25.02	6.28	3.54	0.252	0.49	0.75	0.025	0.0001	Bal.

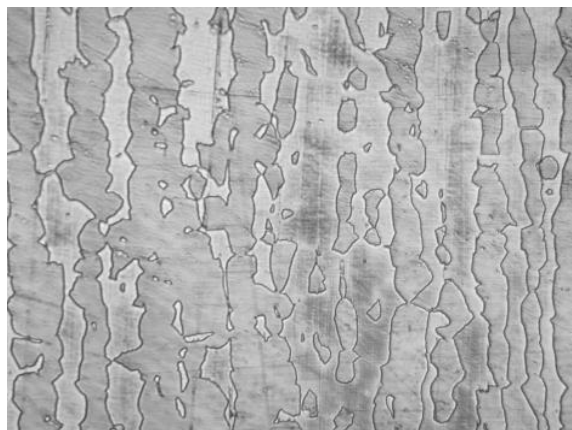


Figure 1. S32750 SDSS metallographic microstructure

2.1 Electrochemical measurements

Electrochemical measurements were performed with a traditional three-electrode cell systems provided by the PARSTAT 2273 electrochemical workstation. The S32750 SDSS samples with hydrogen charging were used as the working electrode (WE), Pt sheet served as the counter electrode (CE), saturated calomel electrode (SCE) as the reference electrode. All potentials in the work are relative to SCE, WE was sealed by epoxy resin with a working area of 1 cm^2 followed by grinding sequentially with SiC papers from 180 to 2000 grit, and washed with deionized water and rinsed by anhydrous ethanol, and then dried in a desiccator. The corrosive medium used in the study was a 3.5% NaCl solution. During the measurements, the solution temperature was maintained at $25 \pm 1^\circ\text{C}$ using a HH-6 type water bath.

Hydrogen was introduced into the S32750 SDSS samples by cathodic current method under galvanostatic condition in the $1.26 \text{ mmol}\cdot\text{L}^{-1} \text{ Na}_4\text{P}_2\text{O}_7 + 0.5 \text{ mol}\cdot\text{L}^{-1} \text{ H}_2\text{SO}_4$ solution at 25°C . The S32750 SDSS specimens were serially charged at hydrogen charging current densities (HCCDs) of 0, 10, 20, 50 and $100 \text{ mA}\cdot\text{cm}^{-2}$ for 1 hour, respectively.

The electrochemical curves tests of S32750 SDSS samples charged with hydrogen at different current densities were performed, respectively.

Electrochemical impedance spectroscopy (EIS) were carried out using AC signals with an amplitude of 10 mV in the frequency range from 100 kHz to 100 mHz. The measured EIS data was fitted using Zview 3.20 software.

The specimens were immersed in the solution for 1 hour in order to reach a nearly steady-state open-circuit potential values (OCP), and then the potentiodynamic polarization curves are obtained starting from a potential -0.3 to 1.3 V at a scan rate of $1.0 \text{ mV}\cdot\text{s}^{-1}$. The corrosion behavior of S32750 SDSS is evaluated by the absolute value of pitting potential E_b , corrosion current density i_{corr} and corrosion potential E_{corr} established from polarization curves.

The Mott-Schottky curves are obtained by measuring the capacitance of the passive film formed on the S32750 SDSS specimens. The potential was scanned in the range from -0.2 to 0.8 V. An AC excitation signal amplitude is 10 mV in the frequency of 1000 Hz was adopted to the system.

Potentiostatic critical pitting temperature test was taken to evaluate the pitting corrosion resistance of S32750 SDSS specimens with different hydrogen charging condition. The measurement was based on recording the current flowing in the investigated system at an applied constant potential as a function of temperature. The test in the work was applied at a constant potential of 700 mV_{SCE}. The temperature was initially maintained at 30°C 60 seconds and then increased at a constant rate of $1 \pm 0.1 \text{ } ^\circ\text{C}\cdot\text{min}^{-1}$, and the temperature at which the current density exceeded $100 \text{ }\mu\text{A}\cdot\text{cm}^{-2}$ is defined as the critical pitting temperature (CPT). The temperature was controlled by a programmable temperature controller (THCD-09).

3. RESULTS & DISCUSSION

3.1 Effect of HCCDs on open-circuit potential

The OCP of S32750 SDSS with different hydrogen charging current density (HCCD) in 3.5% NaCl solution was shown in Figure 2. It is seen from the curves that the OCP of each specimen shifts gradually to positive direction with the increasing of immersion time, indicating a passive film forms on the sample surface. In the initial stage of immersion, the OCP rapidly shift to positive direction because of a passive films forming rapidly. When the immersion time reaches 500 seconds, the OCP tends to be stable, and a complete passive film gradually forms and covers the sample surface [12-13]. In addition, when the HCCD increases from 0 to $100 \text{ mA}\cdot\text{cm}^{-2}$, the OCP value of each sample is reduced from -0.2 to -0.38 V. The more dynamically, the more negative the OCP, and the higher tendency the corrosion take place [13-14]. Hence, it can be concluded that the hydrogen weaken the stability of passive film and increases the corrosion tendency of S32750 SDSS.

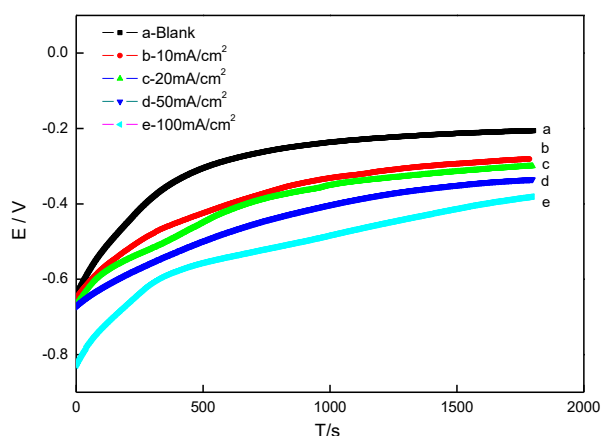


Figure 2. OCP curves of S32750 SDSS for different HCCDs in 3.5% NaCl solution

3.2 Effect of HCCDs on electrochemical impedance spectroscopy

The EIS data corresponding to samples with different HCCDs are provided in Figure 3. Figure

3(a) and 3(b) display the Nyquist and Bode plots, respectively. It can be observed from Figure 3(a) that the diameter of capacitive loops decreases with increasing HCCDs, and it reaches the minimum when the HCCD is up to $100 \text{ mA}\cdot\text{cm}^{-2}$. As shown in Figure 3(b), it may be seen that the phase angle is lower than 90° , moreover, the phase angle of each curve decreases with the increase in HCCD, indicating the corrosion resistance became weaker by hydrogen [15].

An equivalent electrical circuit provided in Figure 3(c) is used to fit the EIS data [16], and the fitted results are listed in Figure 4. In this equivalent electrical circuit, R_s is the electrolyte solution resistance, R_{film} is the resistance of passive film, CPE_{film} is the subsequent passive layer, R_{ct} is the charge transfer resistance, CPE_{dl} represents the capacitance of the passive film including the defects. The non-ideal electric behavior is taken into account by introducing a constant phase element (CPE).

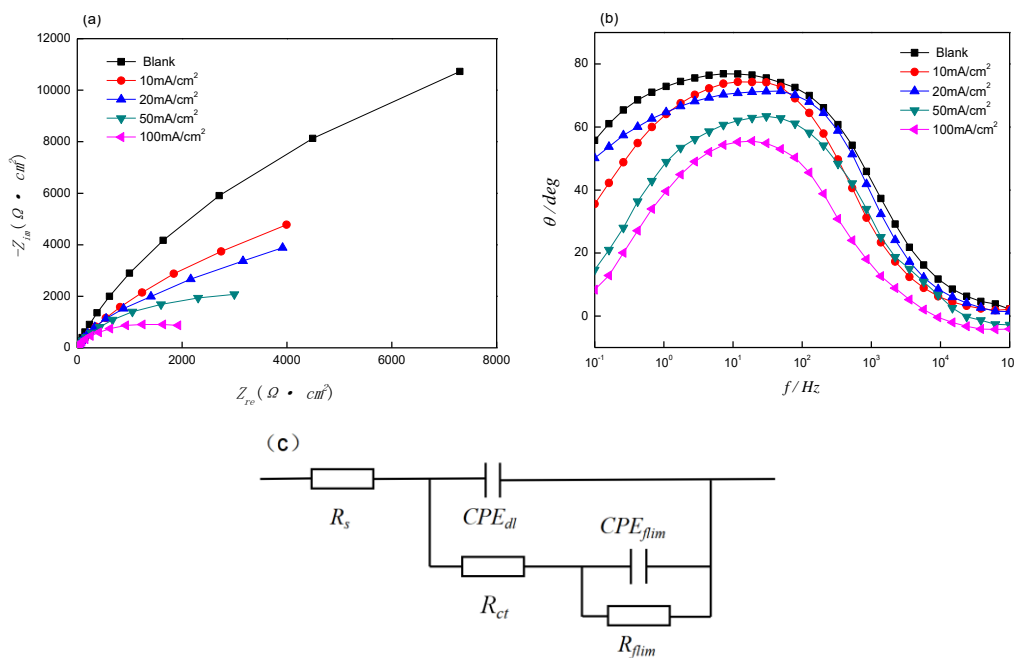


Figure 3. EIS of S32750 SDSS for different HCCDs in 3.5% NaCl solution: (a) Nyquist curves, (b) bode phase value against frequency, and (c) the corresponding simulation circuit

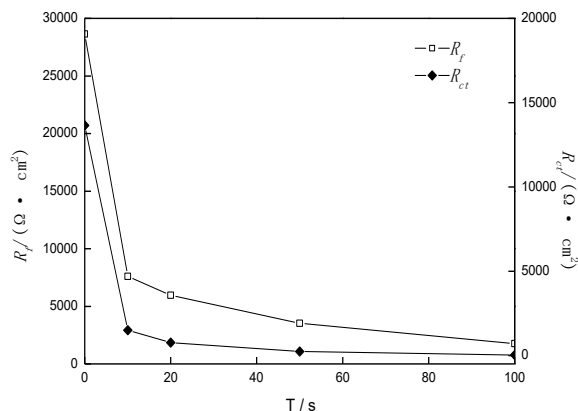


Figure 4. Curves of R_{ct} and R_f for different HCCDs in 3.5% NaCl solution

The larger the values of R_f and R_{ct} , the better the protection of the passive film and the corrosion resistance of material are [17-19]. Figure 4 shows the R_{ct} reduces with the increasing of HCCD, indicating that hydrogen accelerates the electrode reaction and promotes the occurrence of corrosion. R_{film} also decreases with increasing HCCDs, implying that the hydrogen leads to the degeneration and a thickness decrease of the passive film on the surface of the S32750 SDSS sample, the decrease of R_{film} may be attributed to the corrosion rate increase.

3.3 Effect of HCCDs on potentiodynamic polarization

Figure 5 gives the potentiodynamic polarization curves of S32750 SDSS with different HCCDs in 3.5% NaCl solution. It is found that the polarization curve shifts towards the direction of increasing current density as the HCCD increases, meaning that hydrogen accelerates the corrosion rate of S32750 SDSS. It can be also seen that a secondary passivation behavior in S32750 SDSS is significantly weakened when the HCCD increases from 10 to 50 $\text{mA}\cdot\text{cm}^{-2}$, which indicates that the passive film exhibits a double-layer structure: an inner layer rich in Cr_2O_3 and a porous outer layer rich in $\text{Cr}(\text{OH})_3$ [20]. The secondary passivation under the three conditions (10 $\text{mA}\cdot\text{cm}^{-2}$, 20 $\text{mA}\cdot\text{cm}^{-2}$, 50 $\text{mA}\cdot\text{cm}^{-2}$) is all above 0.6 V_{SCE} , which may be related to the reaction:



Where $\text{Cr}_2\text{O}_7^{2-}$ [21] is further transformed into Cr^{6+} . The Cr^{6+} plays an important role in improving the stability of the passive film and enhances the pitting resistance of S32750 SDSS [22]. Since the concentration of hydrogen in the S2750 SDSS is increased after hydrogen charging, the formation of Cr^{6+} is suppressed, and the corrosion resistance of the passive film is reduced. When hydrogen charged at the current density of 100 $\text{mA}\cdot\text{cm}^{-2}$ for 1 hour, the secondary passivation disappears completely, which is because the hydrogen concentration further increases as the increment of HCCDs, and the pH value of the solution decreases, and the reaction in equation (1) almost inhibited [23].

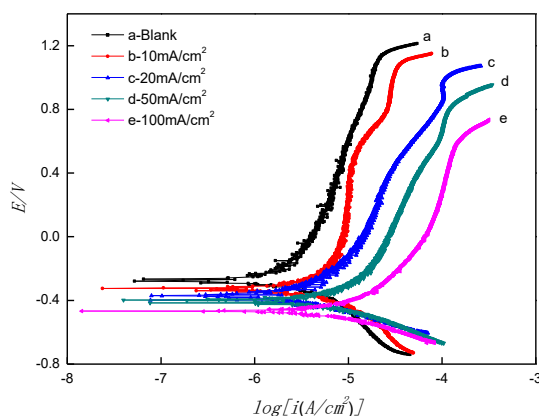


Figure 5. Potentiodynamic polarization curves of S32750 SDSS for different HCCDs in 3.5% NaCl solution and scan rate of $1.0 \text{ mV}\cdot\text{s}^{-1}$

The fitted results of polarization curves are shown in Table 2. It can be seen that, the self-corrosion potential and the pitting corrosion potential decrease, as well as the anode region Tafel slopes

(β_a) and passivity current density increases when the HCCD increases, it is an indication that the corrosion resistance of S32750 SDSS is reduced by hydrogen. The polarization curves results are in agreement with the EIS results.

Table 2. Fitting results of potentiodynamic polarization curves of S32750 SDSS for different HCCDs in 3.5% NaCl solution and scan rate of 1.0 mV·s⁻¹

HCCDs (mA·cm ⁻²)	$E_{corr}(V_{SCE})$	$E_b(V_{SCE})$	$i_{corr}(\mu A \cdot cm^{-2})$	$\beta_a(V/decade)$
Blank	-0.266	1.135	1.445	0.168
10	-0.324	1.064	5.012	0.243
20	-0.369	0.963	8.318	0.318
50	-0.416	0.762	13.489	0.349
100	-0.467	0.582	28.019	0.438

3.4 Effect of HCCDs on Mott-Schottky curves

The semiconducting properties of the passive film formed on the S32750 SDSS with different HCCDs are obtained by capacitance measurements. The relationship between capacitance and applied potential is calculated by the following equations [24-25]:

$$\text{for n-type semiconductor } \frac{1}{C^2} = \frac{2}{\varepsilon\varepsilon_0eN_D} \left(E - E_{fb} - \frac{KT}{e} \right) \quad (2)$$

$$\text{for p-type semiconductor } \frac{1}{C^2} = -\frac{2}{\varepsilon\varepsilon_0eN_A} \left(E - E_{fb} - \frac{KT}{e} \right) \quad (3)$$

where C is the space charge layer capacitance, ε is the dielectric constant of the film (15.6), ε_0 is the dielectric constant of the oxide film (8.854×10^{-14} F·cm⁻¹), and e is the electronic charge (1.602×10^{-19} C). The carrier concentration of the passive film formed on the S32750 SDSS can be defined as the donor densities (N_D) and the acceptor densities (N_A). E is the applied potential, E_{fb} is the flat band potential, K is the Boltzmann constant (1.38×10^{-23} J·K⁻¹), and T is the thermodynamic temperature. N_D and N_A can be estimated from the slope of the straight lines in different zones of $C^{-2} \sim E$ plots.

Figure 6 presents the Mott-Schottky plots of S32750 SDSS with different HCCDs. It can be seen that the value of C^{-2} decreases as the HCCD increases. According to the trend of the plots, the plots can be divided into R_1 and R_2 two capacitance linear change zones. In the R_1 zone, the positive slope is a characteristic of the n-type semiconductor, while, in the R_2 zone, the negative slope is a characteristic of the p-type semiconductor.

The previous studies have shown that the passive film of stainless steel consists of iron oxides and chromium oxides [26-27]. It can be seen that as the potential increases, the slopes of the plots are positive in R_1 where the potential is less than 0.3 V, concluded that the passive film is an n-type semiconductor, at the same time, the space charge layer of Cr oxide in the inner layer of the passive

film is in an enriched state, and the of Fe oxide in the outer layer of the passive film is in a depletion state. Therefore, the passive film behaves as an n-type semiconductor. When the potential is around 0.3 V, the slope of the Mott-Schottky curves in R_2 changes into negative, and the passive film behaves as a p-type semiconductor, in this case, the space charge layer of the Fe oxide on the outer layer of the passive film is in an enriched state, and the Cr oxide in the inner layer of the passive film is in a depleted state [28].

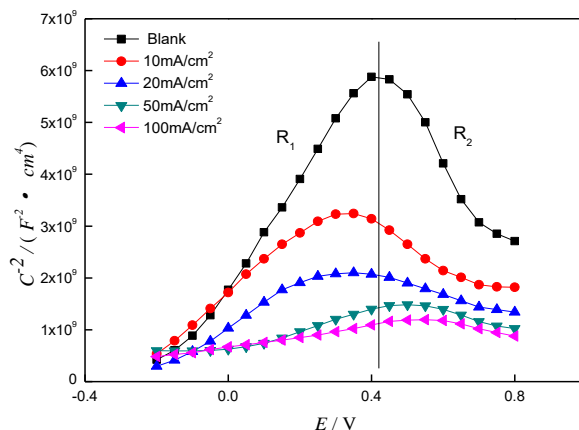


Figure 6. Mott-Schottky plots of S32750 SDSS for different HCCDs in 3.5% NaCl solution and scan rate of $0.5 \text{ mV} \cdot \text{s}^{-1}$

The values of N_D and N_A are calculated according to Equation (2) and (3) by using the slopes of the straight lines of Mott-Schottky plots, and the results are summarized in Table 3.

In all investigated cases, we can see that the concentration values were all in the range of $10^{20} \sim 10^{21} \text{ cm}^{-3}$. Comparing with the blank samples, hydrogen charging affected the values of N_D and N_A , and increase by an order of magnitude. Higher HCCDs and the shift of the N_D and N_A values into the bigger direction were observed, and they eventually reach $5.292 \times 10^{21} \text{ cm}^{-3}$ and $8.694 \times 10^{21} \text{ cm}^{-3}$, respectively. Analysis reveals that both of the hydrogen in the S32750 SDSS sample and the hydrogen in the passive film increases after hydrogen charging, which leading to an increase in the concentration of defects in the passive film and a decrease in the Fermi level. It is suggested that hydrogen promotion of the reaction between the passive film and the solution interface [29], the decrease in the integrity and stability of the passive film. Therefore, the passivity current density decreased, both of dissolution of the passive film and the corrosion reaction accelerated, which agree well with the tendency reflected from the potentiodynamic polarization curves in Figure 5 and the EIS in Figure 3.

Table 3. N_D and N_A of S32750 SDSS for different HCCDs in 3.5% NaCl solution and scan rate of $0.5 \text{ mV} \cdot \text{s}^{-1}$

HCCDs ($\text{mA} \cdot \text{cm}^{-2}$)	$N_A(\text{cm}^{-3})$	$N_D(\text{cm}^{-3})$
Blank	7.686×10^{20}	9.069×10^{20}
10	2.371×10^{21}	1.813×10^{21}

20	3.152×10^{21}	2.451×10^{21}
50	4.872×10^{21}	3.654×10^{21}
100	8.694×10^{21}	5.292×10^{21}

Compared with the blank specimen, the carrier concentration in the passive film increases, leading to an enlarge in the oxygen vacancy concentration in the passive film. According to Macdonald's point defect model [30], when the passive film is in the medium presence of Cl^- , can remarkably facilitate the oxygen vacancies react with Cl^- through the Mott-Schottky pair to generate new oxygen vacancies and metal ion vacancies, and then the generated oxygen vacancies react with other Cl^- , leaving more metal ion vacancies [23]. Between the substrate and the passive film local area metal ion vacancies are easier concentrated, therefore, growth of the passive film will be hinder, and disrupt the dynamic balance between the growth and dissolution of the passive film [15], which would lead to the passive film breakdown in a short period of time. The results further confirmed that hydrogen charging makes the passive film on sample surface more likely to be ruptured, and the corrosion resistance of the S32750 SDSS decreases.

3.5 Effect of HCCDs on critical pitting temperature

The potentiostatic polarization curves provide some important features concerning the pitting corrosion of S32750 SDSS at different HCCDs. Figure 7 shows the potentiostatic polarization curves at a constant potential 0.7 V for the blank specimen without hydrogen and after hydrogen charging at various current densities. The polarization results, repeated three times on each condition, were characterized by a good reproducibility with accurate results. The current density corresponding to the initial application of the 0.7 V polarization potential is very small, indicating that the passive film on the surface of S32750 SDSS is stable in the initial stage. As the temperature rises, the current density increases continuously. When the current density increase to $100 \mu\text{A} \cdot \text{cm}^{-2}$ [31-32], the corresponding temperature at this time is named CPT. It can be seen from the figure that the CPTs of S32750 SDSS for different HCCDs are 72.9°C , 66.7°C , 59.3°C , 50.6°C and 39.2°C , respectively.

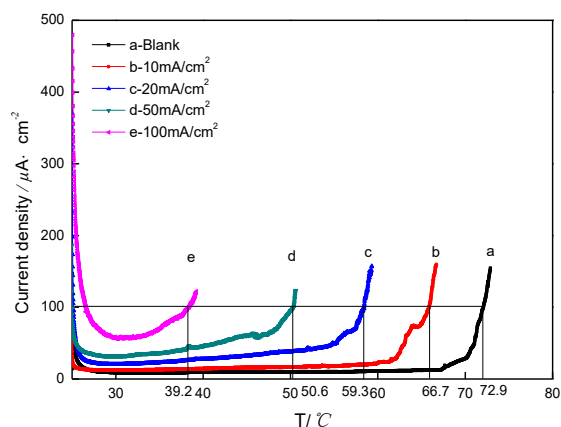


Figure 7. CPT of S32750 SDSS for different HCCDs in 3.5% NaCl solution

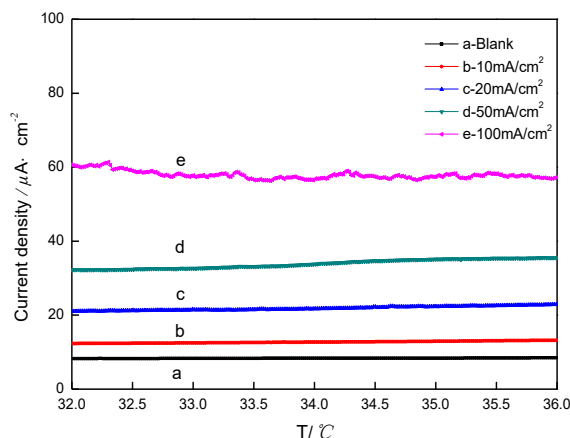


Figure 8. Current density curves of potentiostatic polarization in 3.5% NaCl solution

Figure 8 presents the changes of the potentiostatic polarization current densities (PPCDs) within a specified temperature interval (32°C, 36°C) from Figure 7, and in this interval the changes of the PPCD value are relatively small. Comparing the value of PPCD at different HCCDs, we can find that the blank specimen has the smallest PPCD, because of the surface passive film is stable. As the HCCDs increases, the PPCD of S32750 SDSS continues to increase, and some fluctuations were observed. This is because the corrosion resistance of the passive film on the surface of S32750 SDSS decreases after hydrogen charging, and the diffused hydrogen are oxidized to H^+ , then the H^+ increases the mobile charges in the interface between the passive film and the solution, and hence not only reduces the pH on the electrode interface, but also increases the proportion of OH^-/O^{2-} in the passive film. Therefore, the passive film on sample surface is in an unstable state and susceptible to rupture [33].

The PPCDs increased from approximately $8.3 \mu A \cdot cm^{-2}$ for the blank sample to a value of approximately $56.6 \mu A \cdot cm^{-2}$ for the $100 mA \cdot cm^{-2}$ charged sample, which is approximately increased by 7 times. Passive film is defective, and the defects are often the active sites of pitting corrosion formed. After hydrogen charging, that hydrogen enter the passive film and combine with the defects become hydrogen traps, the rest of the hydrogen that enter the passive film will be ionized in the product film and become hydrogen proton. Defects in the passive film may lead to the accumulation of hydrogen protons and the formations of many small clusters of hydrogen protons [34]. On the one hand, these hydrogen proton clusters reduce the stability of the passive film, and so that the film is prone to rupture. On the other hand, these positively charged hydrogen proton clusters can attract the anions in the solution, especially Cl^- . A large number of Cl^- aggregates on the surface of the passive film, and these aggregated Cl^- are one of the important causes of pitting. With the increase of the HCCDs, the concentration of hydrogen in the passive film increases, and the dissolution of the metal anode is accelerated [35], and the defects in the passive film increases. Since the clusters of hydrogen proton accumulate around the defects, the attraction to Cl^- in the solution becomes stronger, and a higher concentration of Cl^- clusters will be formed and increase the occurrence of pitting corrosion [36].

4. CONCLUSION

This study evaluated the effect of hydrogen on the corrosion behavior of S32750 SDSS in 3.5%NaCl solution. Based on the above results and discussions, the following conclusions can be presented:

(1) The EIS analysis show the R_{ct} and R_{film} decreases with the increase of HCCD, interpreted that hydrogen leads to the degeneration and a thickness decrease of the passive film on the surface of the S32750 SDSS sample.

(2) The potentiodynamic polarization curves reveal that with the increase of HCCD, the pitting corrosion potential and the self-corrosion potential are more negative, and the passivity current density is significantly increased, which is indicated that hydrogen suppressed the reaction associated with the passive film.

(3) The Mott-Schottky curves analysis shows that hydrogen hinders the growth of the passive film and destabilizes the dynamic balance between the growth and dissolution of the passive film, and increases the local vacancy concentration.

(4) The potentiostatic polarization curves displays that the CPT decreases as the HCCD increases, the PCCDs approximately increased by 7 times, and the larger the HCCD is, the value of CPT will be lower.

ACKNOWLEDGEMENTS

The present research is financially supported by Department of Science & Technology of Liaoning Province(No. 20180550348).

References

1. M. Shamanian, M. Mohammadnezhad, M. Amini, A. Zabolian, J. A. Szpunar, *J. Mater. Eng. Perform.*, 24(2015)3118
2. D. Zou, Y. Han, W. Zhang, J. Yu, *J. Wuhan. Univ. Technol.*, 26(2011)183
3. V. D. Cojocaru, D. Răducanu, M. L. Angelescu, A. N. Vintilă, N. Șerban, *JOM-US*, 7(2017)1439
4. C. G. Soares, Y. Garbatova, A. Zayeda, G. Wangb, *Corros. Sci.*, 51(2009) 2014
5. D. Hardie, E. A. Charles, A. H. Lopez, *Corros. Sci.*, 48(2006)4378
6. L. Q. Guo, Y. Bai, B. Z. Xu, W. Pan, J. X. Li, *Corros. Sci.*, 70(2013)140
7. T. L. Zhao, Z. Y. Liu, S. S. Hu, C. W. Du, X. G. Li, *J. Mater. Eng. Perform.*, 26(2017)2837
8. M. Li, L. Q. Guo, L. J. Qiao, Y. Bai, *Corros. Sci.*, 60(2012) 76
9. M. C. Theodoro, V. F. Pereira, P. R. Mei, A. J. Ramirez, *Metall. Mater. Trans. B.*, 46(2015)1440
10. J. R. Gamarra, A. E. Diniz, *J. Braz. Soc. Mech Sci.*, 40(2018)39
11. E. Taban, *J. Mater. Sci.*, 43(2008)4309
12. H. Luo, C. F. Dong, X. Q. Cheng, K. Xiao, X. G. Li, *J. Mater. Eng. Perform.*, 21(2012)1283
13. A. Mostafapour, S. Davoodi, *T. Indian. I. Metals.*, 69(2016)1129
14. S. Choudhary, A. Garg, K. Mondal, *J. Mater. Eng. Perform.*, 25(2016)2969
15. X. Wei, J. H. Dong, J. Tong, Z. Zheng, W. Ke, *Int. J. Electrochem. Sci.*, 8(2013)887
16. P. Vijay, A. Upadhyaya, *T. Indian. I. Metals.*, 61(2008)255

17. X. Li, H. Y. Chen, P. M. Chen, C. X. Qing, H. Y. Li, *J. Mater. Eng. Perform.*, 26(2017)2102
18. E. Husain, A. A. Nazeer, J. Alsarraf, K. Al-Awadi, M. Murad, A. Al-Naqi, A. Shekeban, *J. Coat. Technol. Res.*, (2018)1
19. L. Hamadou, A. Kadri, N. Benbrahim, *Appl. Surf. Sci.*, 252(2005)1510
20. M. V. Cardoso, S. T. Amaral, E. M. A. Martini, *Corros. Sci.*, 50(2008)2429
21. V. B. Singh, M. Ray, *J. Mater. Sci.*, 42(2007)8279
22. D. Marijan, M. Gojić, *J. Appl. Electrochem.*, 32(2002)1341
23. H. B. Li, Z. H. Jiang, H. Feng, Q. Wang, W. Zhang, G. W. Fan, G. P. Li, L. Y. Wang, *Int. J. Electrochem. Sci.*, 10(2015)1616
24. F.R. Attarzadeh, N. Attarzadeh, S. Vafaeian, A. Fattah-Alhosseini, *J. Mater. Eng. Perform.*, 25(2016) 4199
25. A. Fattah-Alhosseini, O. Imantalab, F. R. Attarzadeh, *J. Mater. Eng. Perform.*, 25(2016)4478
26. M. Yeganeh, M. Eskandari, S. R. Alavi-Zaree, *J. Mater. Eng. Perform.*, 26(2017) 2484
27. J. G. Yu, J. L. Luo, P. R. Nprton, *Electrochim Acta.*, 47(2002)1527
28. N. B. Hakiki, S. Boudin, B. Rondot, M. D. C. Belo, *Corros. Sci.*, 37(1995)1809
29. M. F. Montemor, M. G. S. Ferreira, N. E. Hakiki, M. D. C. Belo, *Corros. Sci.*, 42(2000)1635
30. D. D. Macdonald, *J. Electrochem. Soc.*, 139(1992)3434
31. R. Brigham, E. Tozer, *Corrosion*, 29(1973)33
32. R. Brigham, E. Tozer, *Corrosion*, 30(1974)61
33. S. Pyuna, C. Lima, R. A. Oriani, *Corros. Sci.*, 33(1992)437
34. Q. Yang, L. J. Qiao, S. Chiovelli, *Corrosion*, 54(1998)628
35. D. Wallinder, G. Hultquist, B. Tveten, E. Hörnlund, *Corros. Sci.*, 43(2001)1267
36. L. J. Qiao, J. L. Luo, *Corrosion*, 54(1998) 281